$t W^-$ mode of single top quark production

Tim M. P. Tait*
Argonne National Laboratory, Argonne, Illinois 60439
(Received 15 September 1999; published 21 December 1999)

The $t W^-$ mode of single top quark production is proposed as an important means to study the weak interactions of the top quark. While the rate of this mode is most likely too small to be observed at run II of the Fermilab Tevatron, it is expected to be considerably larger at the CERN LHC. In this article the inclusive $t W^-$ rate is computed, including $\mathcal{O}(1/\log m_t^2/m_b^2)$ corrections, and when combined with detailed Monte Carlo simulations, including the top quark and W decay products, indicates that the $t W^-$ single top quark process may be extracted from the considerable $t\bar{t}$ and $W^+ W^- j$ backgrounds at low luminosity runs of the LHC.

PACS number(s): 14.65.Ha, 12.39.Fe, 12.60−i

I. INTRODUCTION

The discovery of the top quark at the Fermilab Tevatron [1] completes the fermionic sector of the standard model (SM) of particle physics. However, many questions regarding the top quark remain, and require further investigation to be settled. The primary question is whether or not the top quark is ''just another quark,'' or if its large mass is indicative that it is something more. The top quark's enormous mass may be a clue that it plays a special role in electroweak symmetry breaking (EWSB), and many of the proposed extensions of the SM explain the large top quark mass by allowing the top quark to participate in modified or nonstandard dynamics [2], connected to the physics which provides the mass of the W and Z bosons. This intriguing hypothesis is best explored by careful study of top quark observables. In particular, single top quark production, as a measure of the top quark's electroweak interactions, is an excellent place to look for new physics related to the EWSB [3].

Single top quark production proceeds through three distinct modes at a hadron collider. The choice of the word ''mode,'' as opposed to ''sub-process,'' is motivated by the fact that each process has different initial and final states, and thus they are in principle separably measurable. The t-channel W-gluon fusion mode [4–7] involves the exchange of a space-like W boson between a light quark and a bottom (b) quark inside the incident hadrons, resulting in a jet and a single top quark. Its rate is rather large at both the Fermilab Tevatron and the CERN Large Hadron Collider (LHC). The s-channel W^* mode [8] involves production of an off-shell, time-like W boson, which then decays into a top and a bottom quark. It has a relatively large rate at the Tevatron, but is comparatively small at the LHC because it is driven by initial state anti-quark parton densities. Finally, the $t W^-$ mode of single top quark production involves an initial state b quark emitting a (close to) on-shell W^- boson, resulting in a $t W^-$ final state. Because of the massive particles in the final state, this mode has an extremely small rate at the Tevatron, but is considerable at the LHC where more partonic energy is available.

Each mode has rather distinct event kinematics, and thus is potentially observable separately from each other [6]. In fact it has been shown [3,9] that each mode is sensitive to different types of new physics, with the $t W^-$ mode distinct in that it is sensitive only to physics which directly modifies the W-t-b interaction from its SM structure. This distinction is a result of the fact that in this mode both the top quark and the W are directly observable, whereas in the other two modes the W bosons are virtual, and thus those processes may receive contributions from exotic types of charged bosons or flavor changing neutral current (FCNC) operators involving the top quark. Even without invoking additional particles or FCNC interactions, the three modes provide complimentary information about the W-t-b interaction by probing it in different regions of momentum transfer. The t-channel and s-channel processes study the vertex when the W boson is space-like or time-like, respectively, and the fermions are (approximately) on shell. The $t W^-$ mode involves the interaction when the W boson is on shell, and one of the fermion lines is off shell. These considerations are compelling reasons to examine the three modes of a single top quark separately, to extract the maximum possible information from single top quark production.

This article contains a detailed study of the $t W^-$ mode of single top quark production with the intent to observe this process for its own sake. Previous analyses focused on this process as a background to heavy Higgs boson decays ($h \to W^+ W^-$) [10] or combined all three single top quark modes together into one signal [11,12]. For the reasons stated above, it is also very important to study the $t W^-$ mode independently from the other single top quark processes. The presentation is arranged as follows. In Sec. II, the inclusive $t W^-$ rate is computed, including large logarithmic corrections of $\mathcal{O}(1/\log m_t^2/m_b^2)$. In Sec. III a Monte Carlo simulation of the signal and the major backgrounds is discussed for the LHC collider, and it is demonstrated that the $t W^-$ signal may be observed with about 1 fb^{-1} of collected data. A summary of the results are given in Sec. IV. Finally, the helicity amplitudes for the signal process at leading order (LO), including all decays, are presented in the Appendix.

*Electronic address: tait@anl.gov

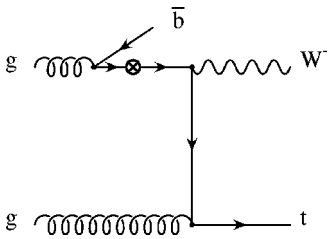

FIG. 1. The underlying picture for production of $t\,W^-$ at a pp or $p\bar{p}$ collider. The crossed circle on the bottom quark line anticipates the improvement of the perturbation series by resumming the $g\to b\,\bar{b}$ portion of the interaction into a b parton density.

II. INCLUSIVE $t\,W^-$ RATE

A. Leading order $2\to2$ contributions

Before turning to the details of how the $t\,W^-$ process may be observed against the background, it is necessary to discuss the inclusive rate of this process at a hadron collider. As is the case with the t-channel single top quark mode [5], the $t\,W^-$ rate involves finding a b quark inside one of the incident (anti-)protons. The underlying picture is actually that a gluon (g) in one of the protons splits into a $b\,\bar{b}$ pair, with one of these bottom quarks taking part in the hard scattering, as is shown in Fig. 1. In order to facilitate the discussion below, only $t\,W^-$ production will be considered, and not $\bar{t}\,W^+$ production. It should be clear how the remarks on single *top quark* production may also be applied to single *top antiquark* production with an appropriate switch of $b\leftrightarrow\bar{b}$, $t\leftrightarrow\bar{t}$, and $W^\pm\leftrightarrow W^\mp$.

One could imagine computing the inclusive $t\,W^-$ rate from a gluon-gluon initial state, such as the one shown in Fig. 1. However, this picture results in a perturbative expansion that is spoiled by the kinematic region in which the produced $\bar{b}$ quark is approximately collinear with the incoming gluon, which produces a contribution containing large logarithms of the form $\alpha_S\log m_t^2/m_b^2$, which for $m_t\sim175$ GeV, $m_b\sim5$ GeV, and $\alpha_S\sim0.1$ is overall of order 1. In fact, the nth order correction to the process always contains a collinear piece which behaves as $(\alpha_S\log m_t^2/m_b^2)^n$, spoiling the perturbative description.

A convergent perturbative expansion is restored by resumming these logarithms into a bottom quark parton distribution function (PDF) [13], which is unlike the usual light parton PDF's in that it is perturbatively derived from the gluon distribution function. Thus, the LO contribution to inclusive $t\,W^-$ production is best considered to arise from Feynman diagrams such as those shown in Fig. 2,[1] which treat the bottom quark as a parton.

This reordering of the perturbation series improves its convergence, and allows an accurate estimation of the inclusive cross section. In fact, this two particle to two particle ($2\to2$) description also represents the most important part of the $t\,W^-$ kinematics, because the dominant kinematic configuration is one in which the $\bar{b}$ is collinear with its parent gluon [5]. However, since it effectively integrates out the $\bar{b}$ momentum, and approximates it as collinear with the parent hadron, this $2\to2$ process does not accurately describe the situation when the $\bar{b}$ has large transverse momentum (p_T). In this region, a description based on the original $2\to3$ process is more appropriate, and since this is the situation in which the $\bar{b}$ is not collinear with the incoming gluon, it is well defined in perturbation theory. Thus, we will see that while it is not possible to compute kinematic distributions in the region in which the p_T of the $\bar{b}$ is small using standard perturbation theory, it is possible to compute the inclusive rate for the process with $p_T^b>p_T^{cut}$, as long as p_T^{cut} is chosen large enough that the perturbative description remains valid.

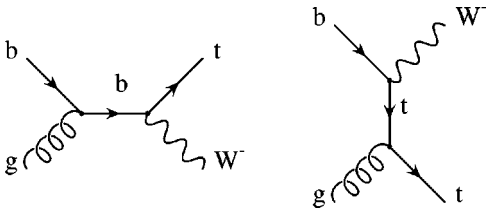

FIG. 2. Feynman diagrams for the $t\,W^-$ mode of single top quark production after resumming large logarithms into a gluon PDF: $g\,b\to t\,W^-$.

B. $\mathcal{O}(1/\log m_t^2/m_b^2)$ $2\to3$ corrections

Though the complete next-to-leading order (NLO) QCD corrections are still underway, the prediction for the inclusive $t\,W^-$ rate may be improved over the LO result by including the $\mathcal{O}(1/\log m_t^2/m_b^2)$ corrections coming from Feynman diagrams such as those in Fig. 3. These diagrams may be separated into three classes. Figure 3a contains a representative diagram which contains the collinear $\mathcal{O}(1/\log m_t^2/m_b^2)$ behavior under study. Figure 3b corresponds to a class of corrections that include contributions which look like $t\,\bar{t}$ production followed by the decay $\bar{t}\to W^-\bar{b}$. The diagram of Fig. 3c contains a separate $\mathcal{O}(\alpha_S)$ correction that involves neither potentially on-shell $\bar{t}$ quarks nor large logarithms. By representative, it is meant that these diagrams are examples of the three categories which contain the complete set of eight tree level $g\,g\to t\,W^-\bar{b}$ matrix elements.

There are two subtle points that must be carefully dealt with when including these corrections. The first is that when the b PDF was defined, the collinear contributions from these diagrams were already resummed into what we called the LO contribution. Thus, in order to avoid double-counting this collinear region one must subtract out this portion. This may be expressed by writing the full cross section for $A\,B\to t\,W^-$ as

$$\sigma_{tW}=\sigma^0(A\,B\to t\,W^-)+\sigma^1(A\,B\to t\,W^-\bar{b})-\sigma^S(A\,B\to t\,W^-\bar{b}), \tag{1}$$

[1]The helicity amplitudes for this $2\to2$ contribution, including the top quark and W decays, can be found in the Appendix.

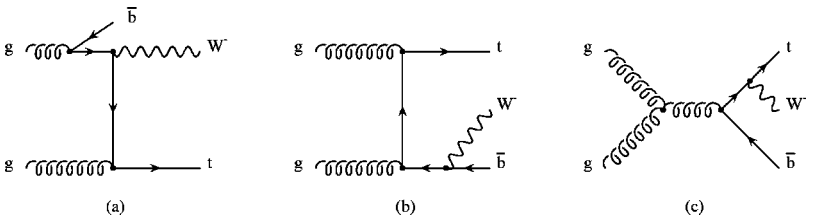

FIG. 3. Representative Feynman diagrams for corrections to the $t\,W^-$ mode of single top quark production corresponding to (a) large logarithmic corrections associated with the b PDF, (b) LO $t\,\bar{t}$ production followed by the LO decay $\bar{t}\to W^-\bar{b}$, and (c) pure α_S corrections.

with the individual terms given by,

$$\sigma^0(A\,B\to t\,W^-)=\int dx_1\,dx_2\{f_{g/A}(x_1,\mu)\,f_{b/B}(x_2,\mu)\times\sigma(b\,g\to t\,W^-)+f_{b/A}(x_1,\mu)\times f_{g/B}(x_2,\mu)\,\sigma(g\,b\to t\,W^-)\}$$

$$\sigma^1(A\,B\to t\,W^-\bar{b})=\int dx_1\,dx_2 f_{g/A}(x_1,\mu)\times f_{g/B}(x_2,\mu)\,\sigma(g\,g\to t\,W^-\bar{b})$$

$$\sigma^S(A\,B\to t\,W^-\bar{b})=\int dx_1 dx_2\{\tilde{f}_{b/A}(x_1,\mu)\times f_{g/B}(x_2,\mu)\,\sigma(b\,g\to t\,W^-)+f_{g/A}(x_1,\mu)\,\tilde{f}_{b/B}(x_2,\mu)\times\sigma(g\,b\to t\,W^-)\},\tag{2}$$

where $f_{i/H}(x,\mu)$ represents the parton distribution function for parton i carrying momentum fraction x at scale μ to be found in hadron H. The ''modified b PDF,'' $\tilde{f}_{b/H}$, contains the collinear logarithm[2] and splitting function $P_{b\leftarrow g}$ convoluted with the gluon PDF:

$$\tilde{f}_{b/H}(x,\mu)=\frac{\alpha_S(\mu)}{2\,\pi}\log\left(\frac{\mu^2}{m_b^2}\right)\int_x^1\frac{dz}{z}\left[\frac{z^2+(1-z)^2}{2}\right]f_{g/H}\left(\frac{x}{z},\mu\right).\tag{3}$$

By including this term, the collinear behavior in $\sigma^1(AB\to t\,W^-)$, which was already implicitly included in $\sigma^0(AB\to t\,W^-)$, is removed. Thus, the problem of double-counting the collinear region is resolved.

The second subtle point in evaluating the large logarithmic contributions is that they contain contributions such as those found in Fig. 3b that correspond to LO $g\,g\to t\,\bar{t}$ production followed by the LO decay $\bar{t}\to W^-\bar{b}$. This expresses the fact that as one considers higher orders in perturbation theory, the distinction between $t\,\bar{t}$ production and various types of single top quark production is blurred. However, when considering quantities that are properly defined, these corrections are small, and there is no problem distinguishing these processes. As a matter of bookkeeping, the corrections to $t\,W^-$ production involving an on-shell $\bar{t}$ are more intuitively considered a part of the LO $t\,\bar{t}$ rate, and thus it is important to subtract them out to avoid double counting in this kinematic region. This may be done by noting that in the region where the invariant mass of the $\bar{b}\,W^-$ system, M_{Wb}, is close to the top quark mass, the behavior of the partonic cross section $\sigma(gg\to t\,W^-\bar{b})$ may be expressed as

$$\frac{d\sigma}{dM_{Wb}}(g\,g\to t\,W^-\bar{b})=\sigma^{LO}(g\,g\to t\,\bar{t})\times\frac{m_t\,\Gamma^{LO}(\bar{t}\to W^-\bar{b})}{\pi\,[(M_{Wb}^2-m_t^2)^2+m_t^2\,\Gamma_t^2]}=\sigma^{LO}(g\,g\to t\,\bar{t})\times\frac{m_t\,\Gamma_t\,\mathcal{B}(\bar{t}\to W^-\bar{b})}{\pi\,[(M_{Wb}^2-m_t^2)^2+m_t^2\,\Gamma_t^2]}\to\sigma^{LO}(g\,g\to t\,\bar{t})\,\mathcal{B}(\bar{t}\to W^-\bar{b})\times\delta(M_{Wb}^2-m_t^2)\tag{4}$$

where $\sigma^{LO}(g\,g\to t\,\bar{t})$ and $\Gamma^{LO}(\bar{t}\to W^-\bar{b})$ are the LO cross section and partial width, Γ_t is the inclusive top quark decay width, and $\mathcal{B}$ denotes the branching ratio. The last distribution identity holds in the limit $\Gamma_t\ll m_t$. Having identified this LO on-shell piece, it may now be simply subtracted from $\sigma(g\,g\to t\,W^-\bar{b})$. The advantage to this formulation of the subtraction is that by taking the narrow width limit, one removes all of the on-shell $\bar{t}$ contribution. The interference terms between one of the on-shell $\bar{t}$ amplitudes and an amplitude without an on-shell $\bar{t}$ involve a Breit-Wigner propagator of the form $(M_{Wb}^2-m_t^2+i\,m_t\Gamma_t)^{-1}$, which in the limit of small Γ_t may be expressed as a principle valued integral in M_{Wb}. Following this prescription, and choosing a canonical scale choice of $\mu_0=\sqrt{s}$, where s is the invariant mass of the incoming partons, leads to a large logarithmic correction to the $t\,W^-$ rate of -9.5% at the LHC, which is consistent with previous experience from the W-gluon fusion mode of single top quark production [6].

This problem of the on-shell top quark was dealt with another way in [12], where a cut was applied on M_{Wb}, to exclude the region of $|M_{Wb}-m_t|\leqslant 3\,\Gamma_t$. Following this prescription, one finds a much larger correction of about $+50\%$

[2]This result is derived by including a small (but non-zero) bottom quark mass in the $2\to 3$ matrix elements in order to regulate the collinear divergence occurring in the class of diagrams represented by Fig. 3a.

TABLE I. The LO [with $\mathcal{O}(1/\log m_t^2/m_b^2)$ corrections] rates of $b\,g \to t\,W^-$ (in pb) at the Tevatron run II. The rate of $\bar{t}$ production is equal to the rate of t production.

	CTEQ4L			MRRS(R1)			
m_t (GeV)	$\mu=\mu_0/2$	$\mu=\mu_0$	$\mu=2\mu_0$	$\mu=\mu_0/2$	$\mu=\mu_0$	$\mu=2\mu_0$	$\sigma_{tW}^{(mean)}$
170	0.0645	0.0505	0.0405	0.0760	0.0580	0.0460	0.0545
171	0.0630	0.0490	0.0395	0.0740	0.0565	0.0445	0.0530
172	0.0610	0.0480	0.0385	0.0720	0.0550	0.0435	0.0515
173	0.0595	0.0465	0.0375	0.0700	0.0530	0.0420	0.0500
174	0.0575	0.0450	0.0365	0.0680	0.0515	0.0410	0.0485
175	0.0560	0.0440	0.0355	0.0660	0.0500	0.0395	0.0470
176	0.0545	0.0425	0.0345	0.0640	0.0490	0.0385	0.0460
177	0.0530	0.0415	0.0335	0.0620	0.0475	0.0375	0.0445
178	0.0515	0.0405	0.0325	0.0600	0.0460	0.0365	0.0435
179	0.0500	0.0390	0.0315	0.0585	0.0445	0.0355	0.0420
180	0.0485	0.0380	0.0305	0.0570	0.0435	0.0345	0.0410
181	0.0475	0.0370	0.0300	0.0555	0.0425	0.0335	0.0400
182	0.046	0.0360	0.029	0.0540	0.0410	0.0325	0.0385

to the $t\,W^-$ rate at the LHC. However, this is misleading because the large corrections are mostly coming from the region where the $\bar{t}$ is close to on-shell (though still at least 3 top quark widths away). In other words, the large positive correction comes from the tails of the Breit-Wigner distribution for on-shell $\bar{t}$ production. This can be simply understood by taking the prescription in [12] and varying the cut by increasing the interval about the on-shell $\bar{t}$ region that is excluded. One finds that the correction computed in this way varies quite strongly with the cut, and reproduces the subtraction method we have employed for the cut $|M_{Wb}-m_t| \leqslant 12\,\Gamma_t$. A theoretical advantage of the subtraction method employed here is that when one determines the $t\,\bar{t}$ and $t\,W^-$ rates, one would like to actually fit the data to the sum of the two rates, and thus the subtraction method allows one to simply separate this sum into the two contributions without introducing an arbitrary cutoff into the definition of the separation.

Even if one were to use a cutoff to effect the separation, there is a further problem in employing the cut $|M_{Wb}-m_t| \leqslant 3\,\Gamma_t$ to remove on-shell $t\,\bar{t}$ production. This is that from a purely practical point of view $3\,\Gamma_t \sim 4.5$ GeV, which is much smaller than the expected jet resolution at the Tevatron or LHC. Thus, it is not experimentally possible to impose this definition of the separation between $t\,W^-$ and $t\,\bar{t}$. A more realistic resolution is about 15 GeV [14], which corresponds to a subtraction of $|M_{Wb}-m_t| \leqslant 10\,\Gamma_t$. As we have seen above, this choice of the M_{Wb} cut agrees rather well with our subtraction method result.

In Tables I and II can be found the LO rate (including the large logarithmic corrections described above) of $t\,W^-$ production at the Tevatron and LHC, for various choices of m_t, the CTEQ4L [15] and Martin-Roberts-Ryskin-Stirling set R1 [MRRS(R1)] [16] PDF's, and 3 choices of factorization scale, with the canonical scale choice set to $\mu_0=\sqrt{s}$. These

TABLE II. The LO [with $\mathcal{O}(1/\log(m_t^2/m_b^2)$ corrections] rates for $b\,g \to t\,W^-$ (in pb) at the LHC. The rate of $\bar{t}$ production is equal to the rate of t production.

	CTEQ4L			MRRS(R1)			
m_t (GeV)	$\mu=\mu_0/2$	$\mu=\mu_0$	$\mu=2\mu_0$	$\mu=\mu_0/2$	$\mu=\mu_0$	$\mu=2\mu_0$	$\sigma_{tW}^{(mean)}$
170	33.0	28.2	24.5	39.0	33.0	28.4	30.6
171	32.2	27.5	24.0	38.3	32.5	27.9	30.0
172	31.6	27.1	23.6	37.6	31.8	27.4	29.4
173	31.1	26.6	23.1	38.0	31.3	26.9	28.9
174	30.5	26.1	22.7	36.2	30.7	26.4	28.4
175	29.9	25.6	22.2	35.4	30.1	26.0	27.9
176	29.4	25.2	21.8	34.8	29.6	25.5	27.4
177	28.9	24.7	21.5	34.2	28.9	25.0	26.8
178	23.3	24.2	21.1	33.6	28.4	24.6	26.3
179	27.8	23.7	20.7	33.0	27.9	24.1	25.8
180	27.2	23.3	20.3	32.4	27.4	23.7	25.4
181	26.8	22.9	20.0	31.8	26.9	23.2	24.9
182	26.3	22.5	19.6	31.2	26.4	22.9	24.5

results assume[3] $V_{tb}=1$, $V_{ts},V_{td}=0$ and no decay branching ratios are included. At both Tevatron and LHC, the rate for $\bar{t}\,W^+$ production is equal to the rate of $t\,W^-$ production, and thus the sum of the two rates may be obtained by multiplying the cross sections by 2. From these results, we see that varying the scale by a factor of 2 produces a variation in the resulting cross section of about $\pm 25\%$ at the Tevatron and $\pm 15\%$ at the LHC. This large scale dependence signals the utility in having a full NLO (in α_S) computation of this process in order to have a more theoretically reliable estimate for the cross section.

It is further interesting to examine the dependence of the result on the choice of PDF, as the $t\,W^-$ process is sensitive to the gluon density, which is parametrized differently by the CTEQ4 and MRRS PDF's. This provides one with an estimate of the uncertainty due to the difference in the PDF parametrization. Unlike the light quark distributions, which are rather well determined by deeply inelastic scattering (DIS) data, the gluon PDF is relatively poorly known at large momentum fraction, and thus the two parametrizations can lead to rather different results for the $t\,W^-$ cross section. For $m_t=175$ GeV, comparing at the canonical scale choice, a variation of $\pm 6\%$ at the Tevatron and $\pm 8\%$ at the LHC results when moving from either the CTEQ4L or MRRS(R1) result to the mean of the two. However, care must be taken in drawing firm conclusions from this because these two sets of PDF's are extracted from a very similar collection of experimental data. Thus, this estimate does not accurately reflect the uncertainty in the PDF's coming from the uncertainties in the data from which they are derived.

III. EXTRACTING $t\,W^-$ FROM THE BACKGROUND

In this section we present the results of a Monte Carlo study illustrating how one may extract the $t\,W^-$ signal from the relatively large backgrounds. A top quark mass of $m_t=175$ GeV is assumed. The $t\,W^-$ signature consists of the decay products of an on-shell top quark and W^- boson. The SM top decay is $t\to W^+ b$, and the W bosons may decay either into quarks or leptons. While the hadronic W decays are dominant (with branching ratio 6/9), the leptonic decays are generally cleaner, and energetic leptons provide an excellent trigger at a hadron collider. Thus, it is necessary to consider at least one of the W bosons decaying into leptons. This study will be confined to the case where both W's decay into leptons, $W\to l\nu$ with $l=e,\mu$. This avoids potentially huge QCD backgrounds involving the production of one W boson and two or more jets whose invariant mass happens to lie close to m_W. Thus, the signature contains two relatively hard charged leptons, missing transverse energy ($\not{p}_T$) from the unobserved neutrinos, and a bottom quark from the single top quark decay.

The primary background comes from processes which contain two weak bosons and a bottom quark. This includes partonic processes such as continuum $W^+\,W^-\,b$ (shown in Fig. 4) which involve off-shell top quark exchange. In fact, this process is interesting in its own right as a further test of the W-t-b interaction. However, the lack of an on-shell top quark will make this process quite difficult to distinguish from the backgrounds. There are also important fake backgrounds from processes that are similar to the $t\,W^-$ process, and may be misidentified as such. This includes $t\,\bar{t}$ production, when one of the bottom quarks from a top quark decay is unobserved because it falls outside of the detector coverage. As the inclusive $t\,\bar{t}$ rate is more than an order of magnitude larger than the inclusive $t\,W^-$ rate, this is potentially a serious problem in discovering the $t\,W^-$ process. Another class of potentially important backgrounds is $W^+\,W^-\,j$ production (where j is a light quark or a gluon) which are problematic because of the small but non-zero probability that j may be misidentified as jet containing a bottom quark. It should be noted that this set of backgrounds also includes $Z\,Z\,j$ production, with one Z decaying into charged leptons, and the other into neutrinos. As we shall see, the $W^+\,W^-\,j$ and $W^+\,W^-\,b$ backgrounds are much smaller than either the $t\,W^-$ signal or the $t\,\bar{t}$ background. This is easily understood from the fact that the $W^+\,W^-\,b$ and $W^+\,W^-\,j$ backgrounds are $2\to 3$ production processes of $\mathcal{O}(\alpha_S\,\alpha_W^2)$ (followed by W decays), whereas the signal and $t\,\bar{t}$ background are $2\to 2$ production processes of $\mathcal{O}(\alpha_S\,\alpha_W)$ and $\mathcal{O}(\alpha_S^2)$ respectively, followed by top quark decays with unit branching ratio and the same W decays.

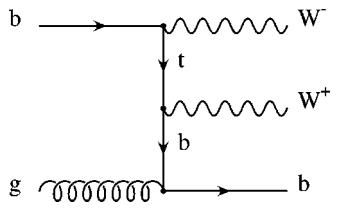

FIG. 4. Illustrative Feynman diagram for the irreducible background, $W^+\,W^-\,b$ production, involving an off-shell top quark. The leptonic decay modes of the W bosons are not indicated here.

The $t\,W^-$ signal, $W^+\,W^-\,b$, and $W^+\,W^-\,j$ backgrounds are simulated at the parton level, at LO in the strong and weak couplings. The matrix elements for the $t\,W^-$ process, including all of the decays, have been computed at the helicity amplitude level, and are presented in the Appendix. Matrix elements for the $W^+\,W^-\,b$ and $W^+\,W^-\,j$ processes have been obtained from the MADGRAPH code [18]. The $t\,\bar{t}$ background is simulated at LO, using the ONETOP code [19]. For all processes, a scale choice of the partonic energy, $\mu=\sqrt{s}$ is chosen, and the CTEQ4L PDF is used with LO running of the strong coupling.[4] Though NLO results for $t\,\bar{t}$ production are currently available [20], we use the LO rates in order to make a fair comparison between this background, the signal,

[3]The inclusion of non-zero V_{ts} and V_{td} has a negligible effect on the cross section, because these parameters are required by low energy processes to be extremely small [17].

[4]The Λ_{QCD} with 5 active flavors appropriate for the CTEQ4L fit is 181 MeV.

TABLE III. The number of signal $t W^-$ events as well as the major backgrounds, for 20 fb^{-1} of integrated luminosity at the LHC after applying cuts described in the text.

Process	Acceptance Cuts	$p_T^{\bar{b}} \leqslant 15$ GeV	b tagging
$t W^-$	25250	13535	8121
$W^+ W^- b$	114	114	68
$W^+ W^- j$	2460	2460	25
$t \bar{t}$	270495	15074	9044

and the other backgrounds, for which NLO results are currently unknown.

In order to be considered observable, the charged leptons and b jet are required to have $p_T \geqslant 15$ GeV, and to lie in the central region of the detector, with rapidity $|\eta| \leqslant 2$. In order to be resolvable as distinct objects, the charged lepton and jet are required to have a cone separation $\Delta R \geqslant 0.4$, where $\Delta R = \sqrt{\Delta\eta^2 + \Delta\phi^2}$, with $\Delta\phi$ the separation in the azimuthal angle, and $\Delta\eta$ the difference in pseudorapidity. In the second column of Table III can be found the number of events passing these cuts for signal and backgrounds at the LHC, assuming 20 fb^{-1} of integrated luminosity.

In order to suppress the large $t \bar{t}$ background, it is desirable to exclude events with more than one b quark at high transverse momentum. The estimation of the effect of this cut on the $t W^-$ signal is somewhat delicate, because, as was discussed in Sec. II, the kinematics of the $\bar{b}$ in the signal events is not calculable in the usual formulation of perturbative QCD. However, the effect of the cut may nonetheless be computed using a technique developed for the W-gluon fusion process [7]. The inclusive $t W^-$ rate computed in Sec. II represents the $t W^-$ rate summed over all p_T of the $\bar{b}$. Further, one can use the $2 \to 3$ description with a sufficiently strong cut on the p_T of the $\bar{b}$ to reliably obtain the cross section when the $\bar{b}$ has a large transverse momentum. Since the inclusive rate is equal to the sum of the rate below the p_T cut and the rate above the p_T cut, one thus computes the signal cross section below the p_T cut from

$$\sigma^{t W^-}(p_T^{\bar{b}} \leqslant p_T^{cut}) = \sigma^{t W^-}_{inclusive} - \sigma^{t W^-}(p_T^{\bar{b}} \geqslant p_T^{cut}). \quad (5)$$

The effect of the cut $p_T^{\bar{b}} \leqslant 15$ GeV on the signal[5] and backgrounds is shown in the third column of Table III. As is indicated, this cut is extremely effective at suppressing the $t \bar{t}$ background, drastically reducing it by about 94%, while eliminating only about 47% of the signal rate.

The $W^+ W^- j$ background has been simulated using the exact matrix elements for $q \bar{q} \to W^+ W^- g$ and $q g \to W^+ W^- q$, which is appropriate for high energy jets. However, it is expected that this background may receive further contributions from initial and final state showering and fragmentation, which have not been included in our estimate. Thus, in order to be conservative, we include b tagging in our search to select events containing a bottom quark. The b-tagging efficiency is estimated by assuming a 60% probability of correctly identifying a bottom quark passing the acceptance cuts described above. The probability of mistagging a light quark[6] or gluon is assumed to be 1%. The effect of this requirement is indicated in the final column of Table III.

One may now estimate the ability of the LHC to study the $t W^-$ process. The significance of the signal over the background is defined as the number of signal events divided by the square root of the number of background events. As the total number of events satisfying our search criterion is large, this approximation based on Gaussian statistics is justified. From the final column of Table III, the significance at the LHC with 20 fb^{-1} of integrated luminosity is seen to be 84.9, indicating that even with a relatively small amount of data the LHC will be able to identify the signal from the background. An alternative presentation is that the LHC will observe the $t W^-$ mode of single top quark production at the 5σ level with less than 1 fb^{-1} of data. In comparison, at the Tevatron run II with 2 fb^{-1}, it is found that after applying the acceptance and $p_T^{\bar{b}}$ cuts, the signal rate is expected to be slightly less than 1 event, thus indicating that another search strategy must be employed in order to observe $t W^-$ at the Tevatron.

IV. CONCLUSIONS

This article is the first proposal to separately study the $t W^-$ mode of single top quark production for its own sake. The inclusive rate has been computed, including the large logarithmic corrections from the definition of the bottom quark PDF. This procedure requires some attention because of potential problems with double-counting both the region where the $\bar{b}$ quark is collinear with the incident gluon, and with $t \bar{t}$ production. After appropriate subtractions, the corrections to the $t W^-$ rate are determined, and it is found that the net correction is about -10% at the LHC.

A full parton-level event simulation has been completed at the LHC, including the decay products from the top quark and W bosons. The decay mode in which both W bosons decay into leptons has been identified as a signature with a relatively small QCD jet background, though other decay modes are also potentially interesting. The $t \bar{t}$ rate is found to be a serious background, but it may be reduced by applying simple cuts to extract the signal from the background. After applying these cuts, it is found that a 5σ observation of the $t W^-$ signal is possible at very low luminosities at the LHC. Turning this around, one finds a statistical error of about 1%

[5]Since this cut restricts the p_T of the $\bar{b}$ to be small, we continue to simulate the signal rate from the $2 \to 2$ process (followed by decays) described in the Appendix, which makes the approximation $p_T^{\bar{b}} = 0$.

[6]The probability of misidentifying a charm quark as a bottom is closer to 15%. However, as the $W^+ W^- c$ portion of the already small $W^+ W^- j$ background is only about 7%, this is of negligible significance.

in the measured cross section at the LHC with 20 fb^{-1}. This error is much smaller than the theoretical uncertainty of $\pm 15\%$ from the scale dependence, which motivates further work to include higher orders of perturbation theory in the $t\,W^-$ rate.

If the top quark has indeed been given a special role in the generation of masses, it is crucial that its interactions be carefully studied in order to learn what properties the underlying theory at high energies must possess. The deviations of the top quark interactions from the SM predictions may represent the best clues on the nature of the EWSB. The $t\,W^-$ rate of single top quark production represents an opportunity to learn about the top quark's weak interactions from a different perspective than is afforded by the *W*-gluon fusion and *W** modes, both because the top quark *and W* are observed, thus allowing one to study the *W-t-b* coupling independently of the possibility of FCNC and heavy particles, and also to probe the *W-t-b* interaction in a different region of momentum transfer from the other two channels. It thus represents an essential means to determine the properties of the top quark.

ACKNOWLEDGMENTS

The author is grateful for invaluable conversations and encouragement from C.-P. Yuan, without which this project would not have been possible, and to B. Harris for reading the manuscript. This work was completed at Argonne National Laboratory, in the High Energy Physics division, and was supported in part by the U.S. Department of Energy, High Energy Physics Division, under Contract W-31-109-Eng-38.

APPENDIX A: HELICITY AMPLITUDES FOR $b\,g \to t\,W^- \to be + \nu_E\,\mu^-\,\overline{\nu}_\mu$

In this appendix, the helicity amplitudes for the $t\,W^-$ process are presented, including the decay products of the *t* and *W*. The helicity amplitudes for the other modes of single top quark production, as well as the $t\,\overline{t}$ background, may be found in [6]. Our conventions for implementing the helicity amplitudes may be found in Appendix A of that work, and are embodied in the two-component ket notation for the spinors:

$$|p_i+\rangle = \sqrt{2\,E_i}\begin{pmatrix}\cos\theta/2\\ e^{i\phi}\sin\theta/2\end{pmatrix},$$

$$|p_i-\rangle = \sqrt{2\,E_i}\begin{pmatrix}-e^{i\phi}\sin\theta/2\\ \cos\theta/2\end{pmatrix} \tag{A1}$$

where E_i, θ, and ϕ refer to the energy, polar angle, and azimuthal angles of the four-momentum p_i. A further notational convenience is to introduce 2×2 Dirac matrices $\gamma_\mu^\pm = (1, \pm\vec{\sigma})$, from which follows the ''slashed'' notation $\not{p}^\pm = p^\mu \gamma_\mu^\pm$. Particle momenta are indicated by the hatted particle label, i.e., $p_{e^+} = \hat{e}^+$.

Purely for the purposes of labelling, we distinguish the decay products of the W^- boson from the W^+ boson by assuming the decays

$$W^- \to \mu^-\,\overline{\nu}_\mu,$$

$$t \to b\,W^+;\quad W^+ \to e^+\,\nu_e. \tag{A2}$$

The other modes of the *W* decays may be easily obtained from this choice by including the appropriate sum over colors for each set of *W* decay products in the final (cross section) result. Namely, each hadronic *W* decay into quarks multiplies the cross section by $N_C = 3$ compared to the leptonic modes presented here.

The results do not include the (negligible) masses of any fermions other than the top quark. This assumption of massless fermions has a profound effect on the helicity structure of the matrix elements because of the left-chiral structure of the *W* interaction. The net result is that only the particular helicity structure $\lambda_{b^i} = -1$, $\lambda_{\mu^-} = -1$, $\lambda_{\overline{\nu}_\mu} = +1$, $\lambda_{e^+} = +1$, $\lambda_{\nu_e} = -1$, $\lambda_{b^f} = -1$ has a non-zero contribution, where $\lambda_n = \pm 1$ when the spin polarization of particle *n* is along (against) its direction of motion. b^i denotes the initial state *b* quark, while b^f denotes the final *b* resulting from the *t* decay. The only remaining polarization to be specified is that of the initial gluon. Denoting the initial gluon spin as $\pm$ for right (left) handed gluons, the two amplitudes may be expressed as

$$\mathcal{M}_1(+) = \left(\frac{\sqrt{2}\,g_W^4\,g_S\,(2E_g)^{-1}}{(\hat{t}_1^2 - m_t^2)(\hat{W}_2^2 - m_W^2 + i m_W\Gamma_W)(\hat{W}_1^2 - m_W^2 + i m_W\Gamma_W)(\hat{t}_2^2 - m_t^2 + i m_t\Gamma_t)}\right)\langle \hat{b}^f - | \hat{\nu}_e + \rangle \langle \hat{\overline{\nu}}_\mu + | \hat{b}^i - \rangle$$
$$\times (m_t^2 \langle \hat{e}^+ + | \hat{g} + \rangle \langle \hat{g} - | \hat{\mu}^- + \rangle - \langle \hat{e}^+ + | \hat{t}_2^- | \hat{g} + \rangle \langle \hat{g} - | \hat{t}_1^- | \hat{\mu}^- + \rangle)$$

$$\mathcal{M}_1(-) = \left(\frac{-\sqrt{2}\,g_W^4\,g_S\,(2E_g)^{-1}}{(\hat{t}_1^2 - m_t^2)(\hat{W}_2^2 - m_W^2 + i m_W\Gamma_W)(\hat{W}_1^2 - m_W^2 + i m_W\Gamma_W)(\hat{t}_2^2 - m_t^2 + i m_t\Gamma_t)}\right)\langle \hat{b}^f - | \hat{\nu}_e + \rangle \langle \hat{\overline{\nu}}_\mu + | \hat{b}^i - \rangle$$
$$\times (m_t^2 \langle \hat{e}^+ + | \hat{g} - \rangle \langle \hat{g} + | \hat{\mu}^- + \rangle - \langle \hat{e}^+ + | \hat{t}_2^- | \hat{g} - \rangle \langle \hat{g} + | \hat{t}_1^- | \hat{\mu}^- + \rangle)$$

$$\mathcal{M}_2(+)=\left(\frac{-\sqrt{2}\,g_W^4 g_S (2E_g)^{-1}}{\hat{b}_1^2(\hat{W}_2^2-m_W^2+im_W\Gamma_W)(\hat{W}_1^2-m_W^2+im_W\Gamma_W)(\hat{t}_2^2-m_t^2+im_t\Gamma_t)}\right)$$
$$\times\langle\hat{b}^f-|\hat{\nu}_e+\rangle\langle\hat{e}^+|\hat{t}_2^-|\hat{\mu}^-+\rangle\langle\widehat{\bar{\nu}}_\mu+|\hat{b}_1^-|\hat{g}+\rangle\langle\hat{g}-|\hat{b}^i-\rangle$$
$$\mathcal{M}_2(-)=\left(\frac{\sqrt{2}\,g_W^4 g_S (2E_g)^{-1}}{\hat{b}_1^2(\hat{W}_2^2-m_W^2+im_W\Gamma_W)(\hat{W}_1^2-m_W^2+im_W\Gamma_W)(\hat{t}_2^2-m_t^2+im_t\Gamma_t}\right)$$
$$\times\langle\hat{b}^f-|\hat{\nu}_e+\rangle\langle\hat{e}^+|\hat{t}_2^-|\hat{\mu}^-+\rangle\langle\widehat{\bar{\nu}s}_\mu+|\hat{b}_1^-|\hat{g}-\rangle\langle\hat{g}+|\hat{b}^i-\rangle \tag{A3}$$

where,

$$\hat{W}_1=\hat{e}^+ +\hat{\nu}_e\,,\quad \hat{W}_2=\hat{\mu}^- +\widehat{\bar{\nu}}_\mu\,,\quad \hat{t}_1=\hat{b}^i-\hat{W}_2\,,\quad \hat{t}_2=\hat{b}^f+\hat{W}_1\,,\quad \hat{b}_1=\hat{b}^i+\hat{g}, \tag{A4}$$

and E_g is the gluon energy, g_S is the strong coupling constant, and $g_W=e/\sin\theta_W$ is the weak coupling. The matrix elements squared, $|\mathcal{M}|^2$, should be summed over final colors and averaged over initial colors, resulting in a factor of 1/6, and averaged over initial spins, giving a further factor of 1/4. As was noted above, this color factor reflects the case where both W bosons decay into leptons. A W decay into quarks further multiplies the cross section by $N_C=3$ for one hadronic W decay, and $N_C^2=9$ if both W's decay into hadrons. The propagators for the (approximately) on-shell $W^\pm$ and top quark have been expressed according to the Breit-Wigner prescription.

[1] CDF Collaboration, F. Abe *et al.*, Phys. Rev. Lett. **74**, 2626 (1995); DØ Collaboration, S. Abachi *et al.*, *ibid.* **74**, 2632 (1995).

[2] Some interesting examples include W. A. Bardeen, C. T. Hill, and M. Linder, Phys. Rev. D **41**, 1647 (1990); C. T. Hill, Phys. Lett. B **345**, 483 (1995).

[3] For a comprehensive introduction, see Tim M. P. Tait, Ph.D. thesis, Michigan State University, 1999, hep-ph/9907462.

[4] S. Dawson, Nucl. Phys. **B249**, 42 (1985); C.-P. Yuan, Phys. Rev. D **41**, 42 (1990); CCAST Symposium 1993, 1993, p. 259; International Workshop on Elementary Particle Physics: Present and Future, Valencia, Spain, 1995, p. 148; in Proceedings of the 5th Mexican Workshop of Particles and Fields, Puebla, Mexico, 1995; R. K. Ellis and S. Parke, Phys. Rev. D **46**, 3785 (1992); G. Bordes and B. van Eijk, Z. Phys. C **57**, 81 (1993); Nucl. Phys. **B435**, 23 (1995); T. Stelzer, Z. Sullivan, and S. Willenbrock, Phys. Rev. D **56**, 5919 (1997).

[5] S. Willenbrock and D. Dicus, Phys. Rev. D **34**, 155 (1986).

[6] D. O. Carlson, Ph.D. thesis, Michigan State University, 1995.

[7] T. Stelzer, Z. Sullivan, and S. Willenbrock, Phys. Rev. D **58**, 094021 (1998).

[8] S. Cortese and R. Petronzio, Phys. Lett. B **253**, 494 (1991); T. Stelzer and S. Willenbrock, *ibid.* **357**, 125 (1995); M. C. Smith and S. Willenbrock, Phys. Rev. D **54**, 6696 (1996); S. Mrenna and C.-P. Yuan, Phys. Lett. B **416**, 200 (1998).

[9] D. O. Carlson and C.-P. Yuan, Workshop on Physics of the Top Quark, Ames, Iowa, 1995, p. 172; T. Tait and C.-P. Yuan, hep-ph/9710372.

[10] G. Ladinsky and C.-P. Yuan, Phys. Rev. D **43**, 789 (1991); S. Moretti, *ibid.* **56**, 7427 (1997).

[11] A. P. Heinson, A. S. Belyaev, and E. E. Boos, Phys. Rev. D **56**, 3114 (1997).

[12] A.S. Belyaev, E. E. Boos, and L. V. Dudko, Phys. Rev. D **59**, 075001 (1999).

[13] J. C. Collins and W.-K. Tung, Nucl. Phys. **B278**, 934 (1986); F. Olness and W.-K. Tung, *ibid.* **B308**, 813 (1988); M. Aivazis, F. Olness, and W.-K. Tung, Phys. Rev. Lett. **65**, 2339 (1990); Phys. Rev. D **50**, 3085 (1994); M. Aivazis, J.C. Collins, F. Olness, and W.-K. Tung, *ibid.* **50**, 3102 (1994).

[14] ATLAS Letter of Intent, Report No. CERN/LHCC/92-4, 1992; CMS Letter of Intent, Report No. CERN/LHCC/92-3, 1992.

[15] CTEQ Collaboration, H. Lai, J. Huston, S. Kuhlmann, F. Olness, J. Owens, D. Sopher, W.-K. Tung, and H. Weerts, Phys. Rev. D **55**, 1280 (1997).

[16] A. Martin, R. Roberts, M. G. Ryskin, and W. J. Stirling, Eur. Phys. J. C **2**, 287 (1998).

[17] Particle Data Group, R. M. Barnett *et al.*, Phys. Rev. D **54**, 1 (1996).

[18] W. F. Long and T. Stelzer, Comput. Phys. Commun. **81**, 357 (1994).

[19] D. O. Carlson and C.-P. Yuan, Phys. Lett. B **306**, 386 (1993).

[20] P. Nason, S. Dawson, and R. K. Ellis, Nucl. Phys. **B303**, 607 (1988); **B327**, 49 (1989); **B335**, 260(E) (1990); W. Beenakker, H. Kuijf, W. L. van Neerven, and J. Smith, Phys. Rev. D **40**, 54 (1989); R. Meng, G. A. Schuler, J. Smith, and W. L. van Neerven, Nucl. Phys. **B339**, 325 (1990); W. Beenakker, W. L. van Neerven, R. Meng, G. A. Schuler, and J. Smith, *ibid.* **B351**, 507 (1991).